

1 **Development and validation of an imprinted polymer based DGT for**  
2 **monitoring  $\beta$ -blocker drugs in wastewater surveillance**

3 Yanying Li<sup>a</sup>, Mingzhe Wu<sup>a</sup>, Xinyu Yin<sup>a</sup>, Yansong Wang<sup>a</sup>, Dongqin Tan<sup>a</sup>, Peng Zhang<sup>b</sup>,  
4 Zhimin Zhou<sup>c</sup>, Degao Wang<sup>a,\*</sup>, Kevin C. Jones<sup>d,\*</sup>, Hao Zhang<sup>d</sup>

5 <sup>a</sup> College of Environmental Science and Engineering, Dalian Maritime University,  
6 Dalian, Liaoning 116023, P. R. China

7 <sup>b</sup> School of Environmental Science and Technology, Shanxi University of Science &  
8 Technology, Xi'an 710021, P. R. China

9 <sup>c</sup> Science and Technology on Underwater Test and Control Laboratory, The 760th  
10 Research Institute of China Shipbuilding Industry Corporation, Dalian, Liaoning  
11 116023, P. R. China

12 <sup>d</sup> Lancaster Environment Centre, Lancaster University, Lancaster, LA1 4YQ, U.K.

13

14 \* Corresponding authors:

15 E-mails: degaowang@dlnu.edu.cn (Degao Wang);

16 k.c.jones@lancaster.ac.uk (Kevin C. Jones).

17

## 18 **Abstract**

19 Wastewater surveillance is an effective and objective approach to monitor contaminant  
20 releases and drug usage in the catchment, the estimation requires accurate measurement.  
21 In this study, a novel diffusive gradients in thin-film (DGT) technique based on  
22 molecularly imprinted polymers (MIPs) for selective measurement of a class of widely  
23 prescribed cardiovascular drugs ( $\beta$ -blockers) in wastewater was developed. The  
24 synthesized MIPs showed strong affinity and selectivity for the target compounds. The  
25 MIP-DGT had large effective capacities, its performance was independent of a wide  
26 range of environmental conditions, including pH (4.58 – 8.89), ionic strength (0.01 –  
27 0.5 M) and dissolved organic matter ( $< 20 \text{ mg L}^{-1}$ ). Biofouling had little effect on the  
28 uptake of target compounds within 7 days. MIP-DGT devices were applied in a Chinese  
29 urban WWTP alongside an auto-sampler. Metoprolol concentrations detected were one-  
30 fold higher than other  $\beta$ -blockers. Concentrations obtained using MIP-DGT were  
31 comparable to the 24 h composite samples using an autosampler. The estimated daily  
32 consumption calculated based on the data obtained with MIP-DGT implied that  
33 metoprolol and propranolol were the most popular  $\beta$ -blockers in the studied area.  
34 Overall, the results in this study demonstrate that the MIP-DGT is a cost-effective,  
35 reliable and efficient tool for *in situ* wastewater monitoring.

36

37 **Key words:**

38 Diffusive gradients in thin-films (DGT);  $\beta$ -blocker drugs; Molecularly imprinted  
39 polymer (MIP); Wastewater monitoring

40

## 41 **1. Introduction**

42 Wastewater-based epidemiology (WBE) is an objective approach used to monitor

43 environmental and public health impacts within a population. It is helpful for medical  
44 research to investigate drug usage and back-estimate regional consumption [1]. The  
45 sampling approach has great influence on the accuracy of wastewater surveillance.  
46 Conventionally, wastewater samples from the influent of wastewater treatment plants  
47 (WWTPs) are collected using active sampling techniques by auto-samplers for 24 h [2].  
48 In some circumstances, grab sampling of snapshot water samples is also employed [3].  
49 During the storage and transport of large volumes of water, some of the target chemicals  
50 may be lost by degradation and/or sorption on suspended particles. Moreover, the  
51 samples captured by these approaches only provide information for the time of sample  
52 collection; episodic contaminant events may be missed, which may lead to inaccurate  
53 estimation in WBE [4]. The auto-sampler instruments are expensive and sometimes are  
54 not easy to access. This restricts the number of locations and frequency of sampling.  
55 Therefore, the development of a cost-effective sampling approach that provides more  
56 representative (time-integrated) information is required.

57 Compared to the aforementioned sampling approaches, passive sampling has a large  
58 number of advantages. The *in situ* sampling does not affect the environment, the loss  
59 of target chemicals is limited during transport. Retained chemicals in the samplers are  
60 preconcentrated, so that no extra pre-treatment procedure is required and the detection  
61 limit decreases. Moreover, time-weighted average (TWA) concentrations of chemicals  
62 obtained are more representative [5]. Passive sampling techniques, such as POCIS  
63 (polar organic chemical integrative sampler), have been applied to WBE in recent years  
64 [6-8]. However, the measurements by POCIS are highly depended on hydrodynamic  
65 conditions in the field deployments. They need to be calibrated and/or corrected for the  
66 effects of flow through laboratory uptake experiments, or kinetic models, or through  
67 the loss of performance reference compounds (PRCs) added to the sampler. In contrast

68 to POCIS, the diffusive gradients in thin-films (DGT) sampler can be used for field  
69 measurements without calibration prior to deployment. The thick diffusive gel layer  
70 which controls the uptake of chemicals minimizes the effect of the diffusive boundary  
71 layer (DBL), such that sampling is not affected by changes in water flow rates (dynamic  
72 conditions) [9]. The measurements using DGT were reported to have higher accuracy  
73 and precision compared to POCIS. The concentrations of 130 pharmaceuticals  
74 measured by both DGT and POCIS samplers in a river showed narrower range of  
75 variation for DGT results than POCIS results [10]. Several studies reported under-  
76 estimations of target compound concentrations in water monitoring using POCIS, due  
77 to using laboratory-derived uptake rates ( $R_s$ ) obtained from the literature, to the field  
78 conditions [11, 12], which has been further proven by studies that using PRCs for  
79 correction [13].

80 Typical DGT devices are comprised of three layers (from back to front) [14]: a binding  
81 resin-impregnated hydrogel layer, a diffusion hydrogel layer, and a protective filter  
82 membrane. These three layers are sandwiched between a plastic base and piston. The  
83 chemicals diffuse through the top two layers and are accumulated in the binding layer.  
84 The DGT measured concentration of the analytes can be calculated based on Fick's first  
85 law of diffusion and expressed as Eq.1:

$$86 \quad C_{\text{DGT}} = \frac{M \Delta g}{D_e A t} \quad (1)$$

87 Where  $M$  stands for the mass of target compound accumulated on the binding gel (ng),  
88  $\Delta g$  is the thickness of diffusion layer (diffusive gel plus filter membrane, cm),  $D_e$  refers  
89 to the diffusion coefficient of the analyte in the diffusion layer ( $\text{cm}^2 \text{s}^{-1}$ ),  $A$  is the  
90 exposure window area of DGT devices ( $\text{cm}^2$ ), and  $t$  is the deployment time (s).

91 Since 2012, the application of DGT has been extended from trace metals and nutrients  
92 to organic contaminants. It has been employed in wastewater monitoring for antibiotics

93 [15], PFAS [16], PPCPs [17], EDCs [18], synthetic musks [19], etc. Its application for  
94 WBE has just started [20]. A binding layer with large capacity for target compounds is  
95 vital for accurate measurement. Several binding resins have been employed for the  
96 detection of organic compounds, such as HLB, XAD-18, XDA-1, activated charcoal  
97 and PEP-2 [21-25]. Binding gels based on these non-selective resins can adsorb  
98 multiple compounds simultaneously, but the effective capacity may be reduced by the  
99 co-adsorption of non-target substances. Moreover, these co-existing substances may  
100 bring interference to the analysis. Hence, a new DGT device with high selectivity could  
101 be advantageous for accurate measurement of specific organic compounds, particularly  
102 in wastewater sampling because of the huge range of co-existing substances present.

103 Molecularly imprinted polymers (MIPs) are a class of synthetic material used to  
104 selectively remove specific target molecules with pre-designed imprinted cavities [26,  
105 27]. Several types of MIPs have been used as DGT binding materials for specific  
106 organic compounds, such as fluoroquinolones antibiotics [28], ciprofloxacin [29],  
107 tetrabromobisphenol [30] chlorophenols [31], 4-chlorophenol [32] and PAHs [33]. The  
108 selectivity, precision and robustness of MIP-based DGT have been demonstrated,  
109 which laid the foundation of this study.

110  $\beta$ -blocker drugs are among the most prescribed pharmaceuticals globally with  
111 significant annual consumption worldwide due to their crucial role in treating  
112 cardiovascular diseases such as angina, arrhythmias, hypertension, and myocardial  
113 infarction [34]. In addition, they may also be abused by athletes to reduce the cardiac  
114 rhythm and farmers to prevent anxiety in animals [35]. They are not fully absorbed by  
115 the body following ingestion, with a large fraction of the drugs being excreted faeces.  
116 Due to their growing consumption and incomplete removal by WWTP [36],  $\beta$ -blockers  
117 have been widely detected in the environment, with concentrations ranging from ng L<sup>-1</sup>

118 <sup>1</sup> to  $\mu\text{g L}^{-1}$  in waters and from 10s to 10000s of  $\text{ng kg}^{-1}$  in soils and sediments [37, 38].  
119 Harmful effects from  $\beta$ -blockers have been reported on fish, algae, and invertebrates.  
120 The drugs could be accumulated in fish and reduce their egg release [39]. Cellular  
121 damage was observed in tissues of clams and oysters after being exposed to metoprolol  
122 and propranolol [40]. After accumulating in food chains, they can be ingested by  
123 humans. Hence, it is important to monitor the usage of  $\beta$ -blockers and evaluate their  
124 consumption. As described above and shown in Table S1, the monitoring methods for  
125  $\beta$ -blockers have mainly been through grab sampling followed by SPE treatment. Most  
126 studies have used adsorption resins, such as HLB for preconcentration [41], although  
127 some studies have used synthesized MIP materials and employed them for  
128 preconcentration [42]. Apart from grab sampling, passive sampling approaches such as  
129 POCIS [43] have been adopted for measuring  $\beta$ -blockers in rivers and WWTP. To  
130 overcome the *ex situ* sampling problems of active sampling and measurement error  
131 induced by  $R_s$  values of POCIS, the DGT technique has also been developed for a large  
132 number of pharmaceuticals, including 3  $\beta$ -blockers (ATL, MTL, PPL) using HLB as  
133 the binding material [44]. However, the analytical interferences in the complex matrices  
134 sampled in WWTPs may be a problem in wastewater surveillance. Moreover, so far  
135 there has been no systematic study or selective measurement specific for the  $\beta$ -blocker  
136 group using DGT.

137 The aims of this study were therefore to synthesize cost-effective MIP material and  
138 develop a selective MIP-DGT sampler for measuring  $\beta$ -blocker drugs in wastewaters.  
139 The binding properties of the MIP materials and the effective capacity of MIP-DGT  
140 devices were evaluated. The performances of MIP-DGT were tested under different  
141 environmental conditions including pH, ionic strength (IS), dissolved organic matter  
142 (DOM) and biofouling in the laboratory. The dependence of diffusive gel thickness and

143 deployment time were also assessed. After systematic assessment, the novel DGT  
144 devices were deployed in an urban WWTP alongside active sampling, to evaluate its  
145 reliability and robustness for measuring  $\beta$ -blocker drugs in wastewater, so as to more  
146 efficiently and accurately support WBE studies.

## 147 **2. Materials and methods**

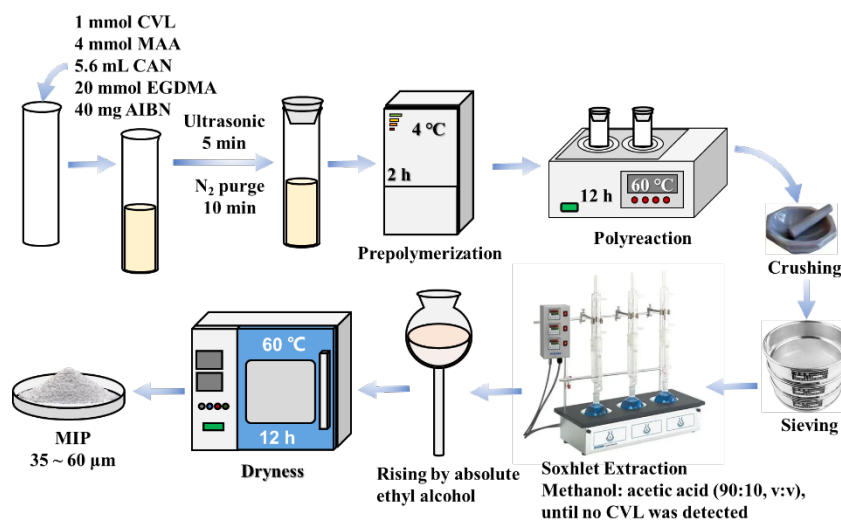
### 148 **2.1 Chemicals and reagents**

149 Standards (> 98%) of atenolol (ATL), acebutolol (ABL), bisoprolol (BSL), betaxolol  
150 (BTL), metoprolol (MTL), nadolol (NDL), propranolol (PPL), sotalol (STL), carvedilol  
151 (CVL), sulfamethazine (SMZ), ractopamine (RTP) and cotinine (COT) were all  
152 purchased from Sigma-Aldrich. ATL-d7 was used as internal standard (IS). Details of  
153 reagents and materials are given in the Supporting Information (SI), physicochemical  
154 properties of all compounds are presented in SI Table S2.

### 155 **2.2 Synthesis and characterization of molecular imprinted polymers (MIP)**

156 The MIP material was synthesized by a bulk polymerization method. CVL was selected  
157 as the template, due to its similar molecular structure to target compounds, low  
158 environmental detection rate [37] and low cost (~\$13/g, HPLC). A schematic diagram  
159 of the synthesis of MIP materials is presented in Fig. 1. In summary, 406 mg CVL (1  
160 mmol) and 0.34 mL (4 mmol) methacrylic acid (MAA) were added into a 50 mL glass  
161 tube containing 5.6 mL ACN, sonicated for 5 min, then the solution was stored in 4 °C  
162 for 4 h. Then 3.8 mL (20 mmol) ethylene glycol dimethacrylate (EGDMA) and 40 mg  
163 2,2'-azobisisobutyronitrile (AIBN) were dissolved in the solution. The mixture was  
164 sonicated and then deoxidized with high purity N<sub>2</sub> for 10 min. The tube was heated at  
165 60 °C in a water bath for 24 h under stirring. The resulting materials were collected,  
166 then crushed and sieved to 35 - 60  $\mu$ m. The template molecules were removed by  
167 Soxhlet extraction with MeOH: HAc = 9: 1 (v:v) until no templates were detected. The

168 wet materials were washed with pure MeOH to remove residual HAc and dried under  
169 vacuum at 60 °C to obtain dry MIP particles. Meanwhile, the non-imprinted polymer  
170 (NIP) materials were prepared by the same procedures described above in the absence  
171 of the templates.



172  
173 Fig. 1. The schematic diagram of the synthesis of MIP materials

174 The size and surface morphologies of the MIP and NIP particles were examined by  
175 scanning electron microscopy (SEM, JEOL LSM-7800F, USA). The surface functional  
176 groups of MIP and NIP were recorded with a Fourier transform infrared spectrometer  
177 (FTIR, Nicolet iS5, USA) in a spectral range of 4000 – 400 cm<sup>-1</sup>. Specific surface areas  
178 were evaluated using the Brunauer-Emmett-Teller (BET) method.

### 179 2.3 Adsorption experiments

180 A series of batch adsorption experiments were carried out to evaluate the binding  
181 properties of the MIP, including the adsorption capacity and binding selectivity. 10 mg  
182 MIP or NIP particles were soaked in a series of 5 mL CVL solutions with concentrations  
183 ranging from 5 - 150 mg L<sup>-1</sup> in 20 mL amber tubes, the tubes were shaken at 150 rpm  
184 in a water bath for 24 h (25 °C). After centrifugation, particles were removed and the  
185 amount adsorbed onto MIP and NIP was determined. The equilibrium adsorption  
186 capacity ( $Q_e$ ) was calculated using the following equation:



187 
$$Q_e = \frac{(C_0 - C_e) \times V}{m} \quad (\text{Eq. 2})$$

188 Where  $C_0$  and  $C_e$  are the initial and equilibrium concentrations ( $\text{mg L}^{-1}$ ) of CVL  
189 respectively.  $V$  (in L) is the solution volume, and  $m$  (in g) is the mass of MIP or NIP.

190 To ensure the selectivity of MIP, competitive adsorption experiments were conducted  
191 by adding 10 mg MIP and NIP particles into 5 mL solutions containing mixed target  $\beta$ -  
192 blockers, together with two competitor compounds (SMZ, highly detectable for co-  
193 existing with  $\beta$ -blockers and has been used as a competitor for testing the selectivity of  
194 MIP material for ATL [45]; RTP, structural analogue) at  $3 \text{ mg L}^{-1}$ . Tubes with solutions  
195 were shaken for 24 h. The distribution coefficient  $K_d$  ( $\text{mL g}^{-1}$ ), selectivity coefficient  
196 ( $\alpha$ ) and relative imprinting coefficient ( $IF$ ) were determined from the following  
197 equations:

198 
$$K_d = \frac{Q_e}{C_e} \quad (\text{Eq. 3})$$

199 
$$\alpha = \frac{K_d (\text{target})}{K_d (\text{competitor})} \quad (\text{Eq. 4})$$

200 
$$IF = \frac{\alpha_{\text{MIP}}}{\alpha_{\text{NIP}}} \quad (\text{Eq. 5})$$

201 where  $Q_e$  is the amount of the compound adsorbed onto the MIP/ NIP ( $\text{mg g}^{-1}$ ) at  
202 equilibrium,  $C_e$  is the concentration of the target compound needed to reach adsorption  
203 equilibrium ( $\text{mg L}^{-1}$ ),  $K_d$  (target) and  $K_d$  (competitor) are the distribution coefficients of  
204 the targets and the interfering compounds,  $\alpha_{\text{MIP}}$  and  $\alpha_{\text{NIP}}$  are selectivity coefficients of  
205 MIP and NIP, respectively.

### 206 **2.3 Gel Preparation and DGT Assemblies**

207 To avoid the possible degradation of agarose gels, which were often used in DGT  
208 devices for organic chemicals, polyacrylamide (PA) gels were used for this work. PA  
209 binding gels were prepared by mixing 1 g MIP material, 10 mL gel solution (provided  
210 by DGT Research Ltd., UK), 60  $\mu\text{L}$  of freshly prepared ammonium persulfate, and

211 initiated by 15  $\mu\text{L}$  of TEMED (N,N,N',N'-tetramethylethylenediamine). The gel  
212 solution was pipetted into two glass plates with 0.25 mm spacer in between and gel was  
213 set under 42 - 45  $^{\circ}\text{C}$  for 40 min. PA diffusive gels were prepared using a 0.5 mm spacer  
214 in the same way as for the binding gels in the absence of the MIP materials. All gels  
215 were hydrated in MQ water for at least 24 h, the thicknesses of the binding gels  
216 expanded to 0.4 mm and diffusive gels to 0.78 mm.

217 Possible adsorption to diffusive gel, filter membrane and DGT moulding has been  
218 assessed in our previous work (data not shown), so the DGT device was assembled with  
219 a 0.4 mm thick MIP binding gel, a 0.78 mm thick PA diffusive gel and a PTFE filter  
220 membrane (0.065 mm) sandwiched between the standard plastic moulding (a base and  
221 a cap).

#### 222 **2.4 Effective adsorption, uptake kinetics and elution efficiencies of DGT**

223 The effective capacities of DGT were measured by deploying DGT devices in 0.01 M  
224 NaCl solutions with concentrations of mixed compounds ranging from 100 to 1000  $\mu\text{g}$   
225  $\text{L}^{-1}$ . Each DGT device was immersed in a 50 mL solution (triplicate) and was shaken  
226 for 24 h. The amount of target compounds taken up by DGT devices were obtained by  
227 measuring the difference between concentration before and after shaking.

228 To investigate uptake kinetics of the target compounds, each DGT device with binding  
229 gel in the front was immersed in 50 mL solution containing 20  $\mu\text{g}$   $\text{L}^{-1}$  of mixed  
230 compounds and 0.01 M NaCl. All solutions were shaken for 24 h, 0.2  $\mu\text{L}$  subsamples  
231 of solution were collected from 5 min to 24 h.

232 The elution efficiencies were evaluated by immersing MIP binding gels separately in  
233 10 mL solutions containing 5 (for laboratory samples) and 0.5 (for field samples)  $\mu\text{g}$   $\text{L}^{-1}$   
234 mixed-compounds and shaken for 24 h. Three different elution solutions were tested:  
235 i) 10% acetic acid (HAc) in methanol (MeOH); ii) acetonitrile (ACN) in MeOH and iii)

236 5% NH<sub>3</sub> in MeOH. Binding gels were eluted with 5 mL of elution solution for 30 min  
237 sonication. For 0.5 µg L<sup>-1</sup> target compounds, the elution were only carried out using 10%  
238 acetic acid (HAc) in MeOH. The elution efficiencies were calculated using the ratio of  
239 masses of target compounds in the eluent to their masses adsorbed on the binding gels.

## 240 **2.5 Time and diffusive layer thickness dependence**

241 To test if the performance of DGT follows the DGT principle, DGT devices were  
242 deployed in a well-stirred solution (pH = 6.5 ± 0.2, 0.01M NaCl, T = 26 ± 0.5 °C)  
243 containing mixed compounds at 10 µg L<sup>-1</sup> for different time periods up to 168 h. The  
244 masses accumulated on the binding gels for different time periods were determined.  
245 DGT devices with various thicknesses of diffusive gels (0.5 to 2.0 mm) were deployed  
246 in a well-stirred 10 µg L<sup>-1</sup> mixed target β-blocker solution for 24 h (pH = 6.4 ± 0.3,  
247 0.01M NaCl, T = 24.1 ± 0.6 °C).

## 248 **2.6 DGT performance tests under different conditions**

249 To investigate if the performances of DGT devices were affected under different  
250 environmental conditions, DGT devices were deployed in 5 µg L<sup>-1</sup> mixed-compound  
251 solutions for 24 h with (a) various pH (ranging from 4 – 9), 0.01 M NaCl, no DOM  
252 addition, T = 26.3 ± 0.3 °C; (b) different ionic strength (IS) (from 0.01 to 0.5 M), pH =  
253 6.4 ± 0.3, no DOM addition, T = 25.2 ± 0.5 °C; (c) DOM (humic acid) ranging from 0  
254 to 20 mg L<sup>-1</sup>, pH = 6.5 ± 0.2, IS = 0.01 M, T = 23.4 ± 0.6 °C.

255 As previously reported, biofilm would form and grow on the surface of the filter  
256 membrane when DGT devices were deployed for a long time. Biofouling could  
257 potentially influence the DGT measurement by interacting with target compounds,  
258 impeding the diffusion or increasing the thickness of the diffusion layer. To investigate  
259 the influence of biofilm on the performance of DGT, fouled filter membranes were  
260 collected from WWTP deployment and reassembled with clean diffusive gels and

261 binding gels. Reassembled DGT devices with clean filters, fouled filters from 7-day  
262 and 14-day deployment were deployed in  $5 \mu\text{g L}^{-1}$  mixed-compound solutions (pH =  
263  $6.8 \pm 0.2$ , IS = 0.01 M, no DOM addition,  $T = 25.8 \pm 0.4 \text{ }^\circ\text{C}$ ) for 24 h.

## 264 **2.9 Application of DGT *in situ* in WWTPs**

265 To test whether MIP-DGT can be used for wastewater surveillance and can be applied  
266 for WBE, a 7-day sampling campaign was conducted in the influent of a WWTP in  
267 Dalian, China in December 2023. An auto sampler (pumping 50 mL every half hour)  
268 was employed together with the deployment of MIP-DGTs (shown in Fig. S4 (a) and  
269 (b)). The 24h composite water samples were collected into glass bottles in duplicate  
270 daily. MIP-DGTs were fixed in a protective plastic cage, then deployed 30 cm under  
271 the water surface in triplicate for 1, 3, 5 and 7 days. After retrieval, DGT devices were  
272 rinsed thoroughly with MQ water and placed in a clean plastic bag before transportation  
273 to the laboratory. Temperature and pH in the influent were recorded every day. The  
274 devices were treated as mentioned above. Details of the extraction procedures and  
275 sample preparations are described in the SI.

## 276 **2.10 Estimated drug consumption based on wastewater-based epidemiology (WBE)**

277 Nicotine is the main addictive substance of tobacco and can be a biomarker in WBE  
278 estimation. Cotinine (COT), a metabolite of nicotine, has a longer half-life than nicotine  
279 and is not affected by dietary factors. It has been reported to be more stable in  
280 wastewater than other human biomarkers [46]. It has been proposed to reflect the  
281 number of inhabitants (inh) served by the WWTP [47]. As MIP-DGT can only measure  
282  $\beta$ -blockers, DGT with HLB binding gels were used to provide TWA COT  
283 concentrations in WWTP. The population served by the WWTP was calculated using  
284 Eq. 5:

$$285 \quad P_{(\text{COT})} = \frac{C_{\text{COT}} \times F}{E} \quad (\text{Eq. 5})$$

286 where  $P_{(\text{COT})}$  is the population estimated according to COT consumption (1000 inh),  
287  $C_{\text{COT}}$  (ng L<sup>-1</sup>) represents the TWA concentration of COT measured by HLB-DGT in a  
288 5-day deployment,  $F$  (m<sup>3</sup> d<sup>-1</sup>) is the average daily flow of the WWTP during 5-day  
289 deployment,  $E$  (mg d<sup>-1</sup> inh<sup>-1</sup>) is the COT discharge coefficient.

290 The consumption of target  $\beta$ -blocker per capita can be estimated using Eq. 6:

$$291 \quad m_i = \frac{C_i \times F \times f_i}{P_{(\text{COT})}} \quad \text{Eq. 6}$$

292 where  $m_i$  stands for daily consumption of target  $\beta$ -blocker  $i$  (mg (1000 inh)<sup>-1</sup> d<sup>-1</sup>),  $C_i$  is  
293 the concentration of compound  $i$  in WWTP measured by MIP-DGT (ng L<sup>-1</sup>),  $f_i$   
294 represents the correction factor for compound  $i$  (shown in Table S8).

## 295 **2.11 Quality assurance /quality control (QA/QC)**

296 All DGT deployments in the laboratory and the WWTP were conducted in triplicate,  
297 results are expressed as the average  $\pm$  standard deviation (SD). Active samples were  
298 collected in duplicate from WWTP and pre-treated with SPE cartridges. Parallel blank  
299 and control samples were performed with laboratory experiments. Field blank DGTs  
300 were used with field applications.

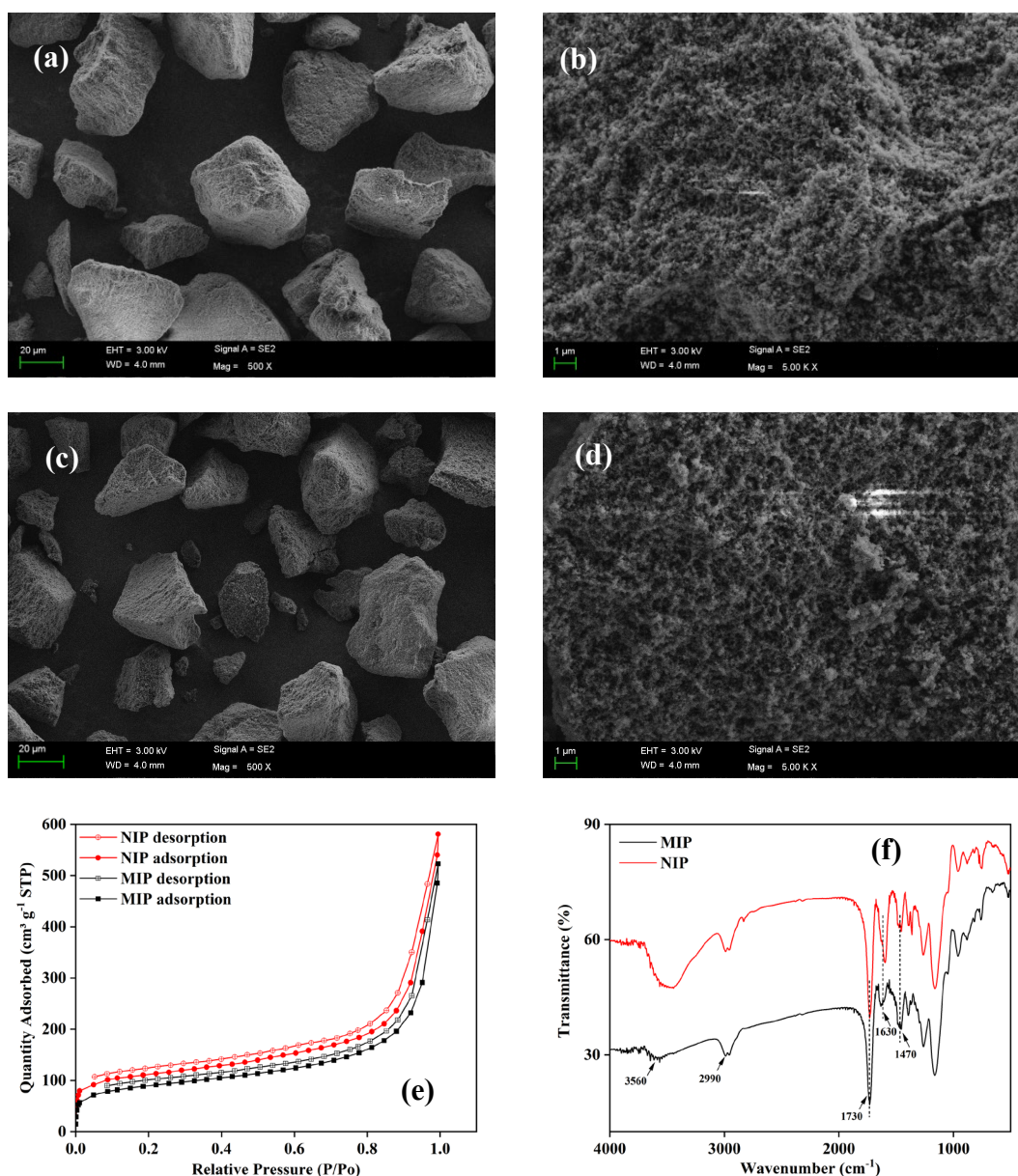
301 The instrumental detection limits (IDLs) for UPLC-MS/MS, method detection limits  
302 (MDLs), diffusion coefficients of target  $\beta$ -blockers, recoveries for DGT and water  
303 samples are given in Table S4.

## 304 **3. Results and Discussions**

### 305 **3.1 Characterization of MIP**

306 The surface morphology of MIP and NIP particles were characterized using scanning  
307 electron microscopy (SEM). As shown in Fig. 2a and c, the particles were irregularly  
308 shaped with a particle size of 35 – 60  $\mu\text{m}$ . Micropores in the material skeleton increased  
309 the specific surface area. High specific surface area of 325.6 m<sup>2</sup> g<sup>-1</sup> (MIP) and 342.8 m<sup>2</sup>  
310 g<sup>-1</sup> (NIP) were obtained through nitrogen adsorption data (shown in Fig. 2e). Fig. 2f

311 shows the results of Fourier transform infrared (FTIR) analysis of the MIPs and NIPs.  
 312 The peaks at 3560 and 1730  $\text{cm}^{-1}$  were attributed to stretching vibration of -OH and  
 313 C=O from MAA. The evidence for successful attachment of MAA and EGDMA  
 314 appeared at 2990  $\text{cm}^{-1}$  for stretching vibrations of C-H, at 1160 and 1260  $\text{cm}^{-1}$  for C-O.  
 315 These characterization results indicated that the MIP and NIP materials were  
 316 synthesized as proposed.

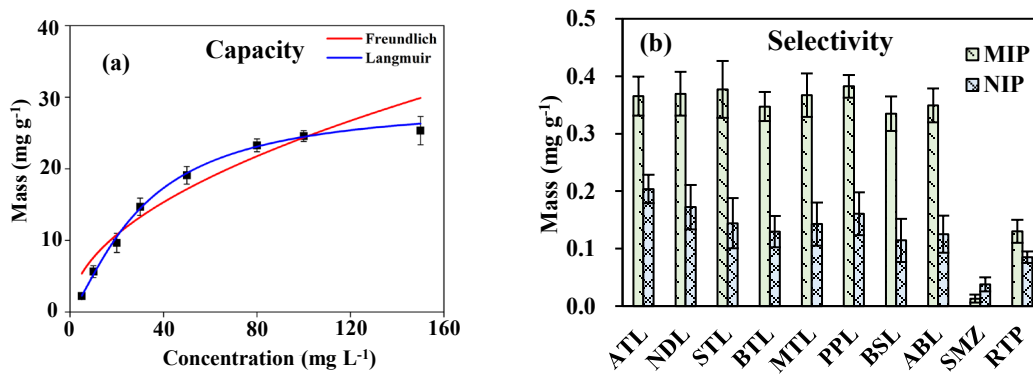


317 Fig. 2. SEM images of MIP at magnification of (a)  $\times 500$ , (b)  $\times 5000$ ; SEM images of  
 318 NIP at magnification of (c)  $\times 500$ , (d)  $\times 5000$ ; (e) Nitrogen adsorption-desorption  
 319 isotherms of MIPs and NIPs; (f) FTIR spectroscopy of MIPs and NIPs.

### 320 **3.2 Adsorption performance of MIPs**

321 The MIP material was immersed in a series of CVL solutions with concentrations  
322 ranging from 5 - 150 mg L<sup>-1</sup>. As presented in Fig. 3(a), the adsorbed masses of CVL  
323 increased rapidly with increasing of test concentration and slowed down when the test  
324 concentration was over 100 mg L<sup>-1</sup>. Langmuir and Freundlich isothermal models were  
325 used to evaluate the maximum capacity of MIP. The results show that the adsorption  
326 process was better fitted with the Langmuir model, indicating a monolayer adsorption  
327 in the material. The adsorption capacity of MIP for CVL was around 29 mg g<sup>-1</sup>.  
328 Comparing to the adsorption capacities (ranging from 0.1 – 31 mg g<sup>-1</sup>) of previously  
329 developed MIP materials using the bulk polymerization method for  $\beta$ -blockers (atenolol,  
330 carvedilol, pindolol, sotalol etc.) [48], the MIPs synthesized in this study have a high  
331 capacity.

332 A highly selective binding material can ensure the effective uptake of target compounds  
333 in complex environments. A competitive adsorption experiment was conducted;  
334 distribution coefficients ( $K_d$ ), selective factor ( $\alpha$ ) and relative imprinting coefficient ( $IF$ )  
335 were used to evaluate the selectivity of MIPs. As shown in Fig. 3(b) and Table S5, the  
336 uptake of target compounds onto the MIP material were much more than that onto the  
337 NIP material, with  $IF$  values ranging from 7.2 – 15.6, which were relatively high values  
338 compared to reports on MIPs for ATL [49, 50]. Meanwhile, the adsorption of interfering  
339 compounds (SMZ and RTP) was much less than the target compounds, indicating that  
340 the MIP material had strong affinity and selectivity to the target  $\beta$ -blockers.

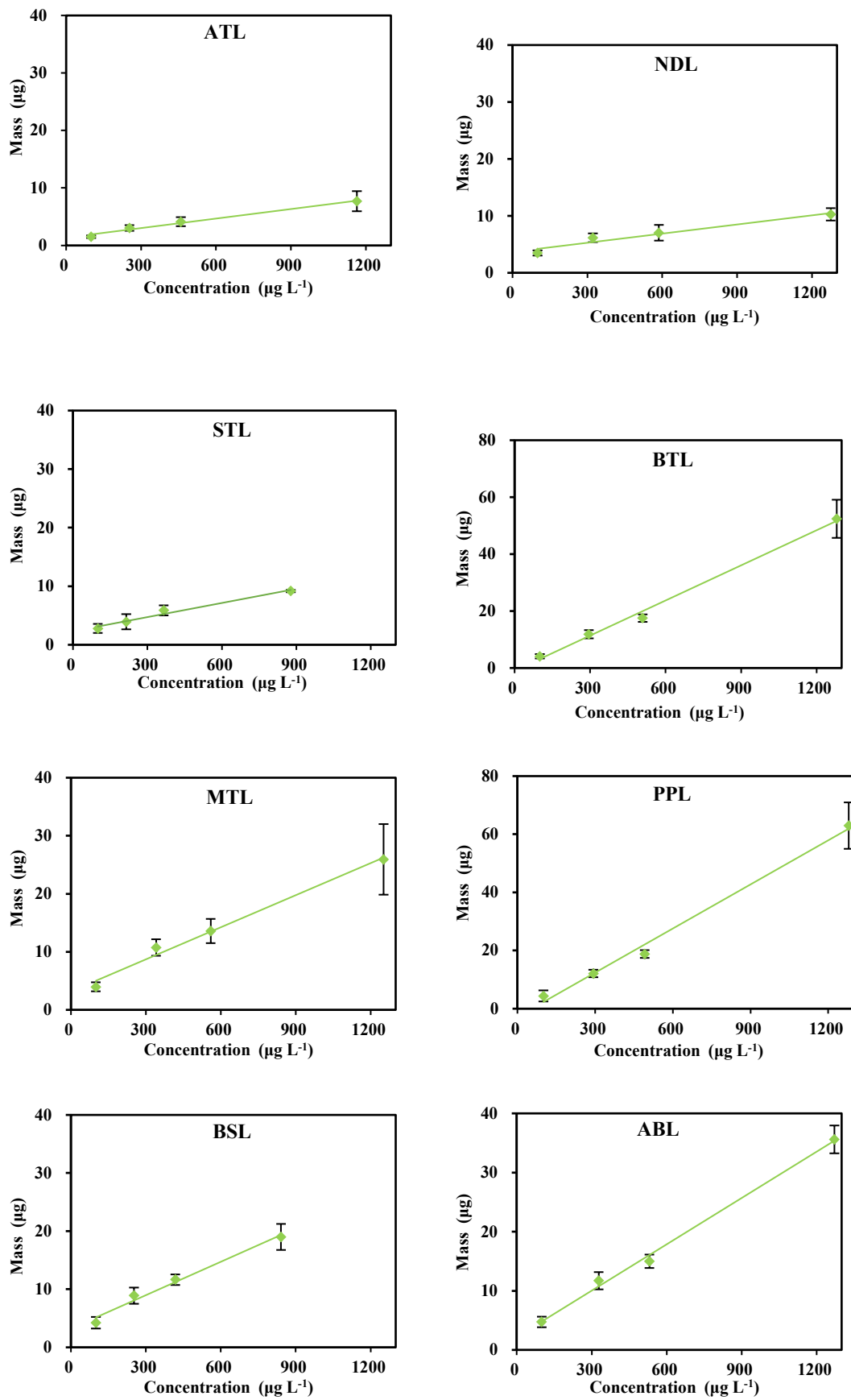


341 **Fig. 3.** (a): Adsorption isotherms of CVL on MIPs and (b): Selectivity of target  $\beta$ -  
 342 blockers on MIP and NIP under competitive conditions.

### 343 3.3 Effective capacity, uptake kinetics and elution efficiency of DGT devices

344 Although the binding material is highly selective, a large capacity for target compounds  
 345 on the binding gel still needed to be evaluated for the measurement in heavily polluted  
 346 environments. The effective capacities of DGT were determined with binding gels in  
 347 the front of the devices with one-side exposed directly to the bulk solution. According  
 348 to Fig. 4, the accumulated masses of all compounds were linearly correlated with the  
 349 increasing solution concentrations. The slopes were steep for 5 target compounds and  
 350 smaller for ATL, NDL and STL, demonstrating a slower uptake of these 3 compounds.  
 351 Within the test concentrations, the effective capacity of all target compounds was at  
 352 least in the range of 8  $\mu\text{g}$  (ATL) - 63  $\mu\text{g}$  (PPL) per device. If the deployment time was  
 353 1 week, as is often the case in WWTP studies, the maximum concentration of  $\beta$ -blockers  
 354 that could be measured ranges from 67 to 530  $\mu\text{g L}^{-1}$ . These were much higher than the  
 355 normal concentrations in WWTP (e.g. ATL: 0.0056 – 11.2  $\mu\text{g L}^{-1}$ , MTL: 0.012 – 8.3  $\mu\text{g}$   
 356  $\text{L}^{-1}$ , PPL: 0.005 – 0.59  $\mu\text{g L}^{-1}$  etc.) [37], and the maximum capacities were not reached  
 357 in this study, confirming that the effective binding capacities of MIP-DGTs were large  
 358 enough for monitoring  $\beta$ -blockers in wastewater.





359 **Fig. 4.** Effective capacities of 8 target  $\beta$ -blockers at different concentrations.

360 As shown in Fig S1, the uptake of target compounds by MIP-DGT increased sharply  
361 and linearly within 60 min, then the uptake rate slowed down slightly. After 24 h of  
362 adsorption, 5 target compounds were taken up by > 90% of the total amount added. The  
363 uptake amount of NDL, STL and ATL after 24 h were 80%, 77% and 42% respectively,  
364 demonstrating there was competition between target compounds.

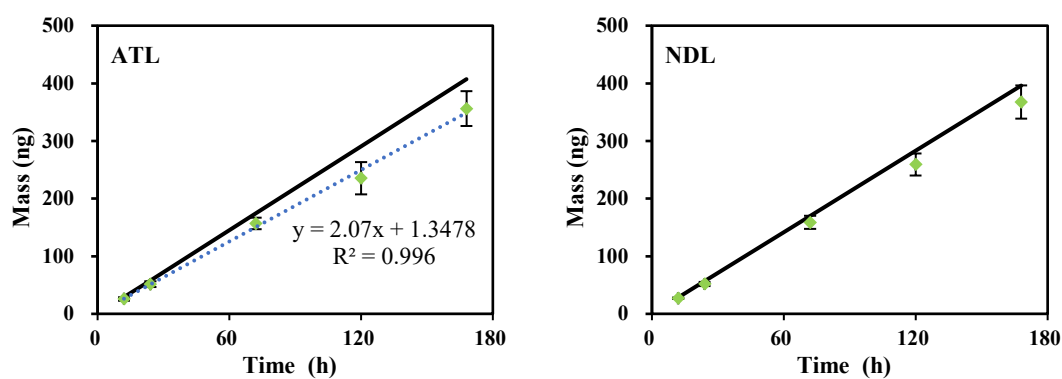
365 According to Fick's first law, the minimum amount of target analytes diffused through  
366 the diffusion layer in the first 5 min was about 1 ng. The actual amounts of target  
367 compounds taken up by MIP binding gel were all > 70 ng (see Figure XX in SI). The  
368 results indicated that the target  $\beta$ -blockers bound onto MIP binding gels sufficiently fast,  
369 which should enable good performance of DGT.

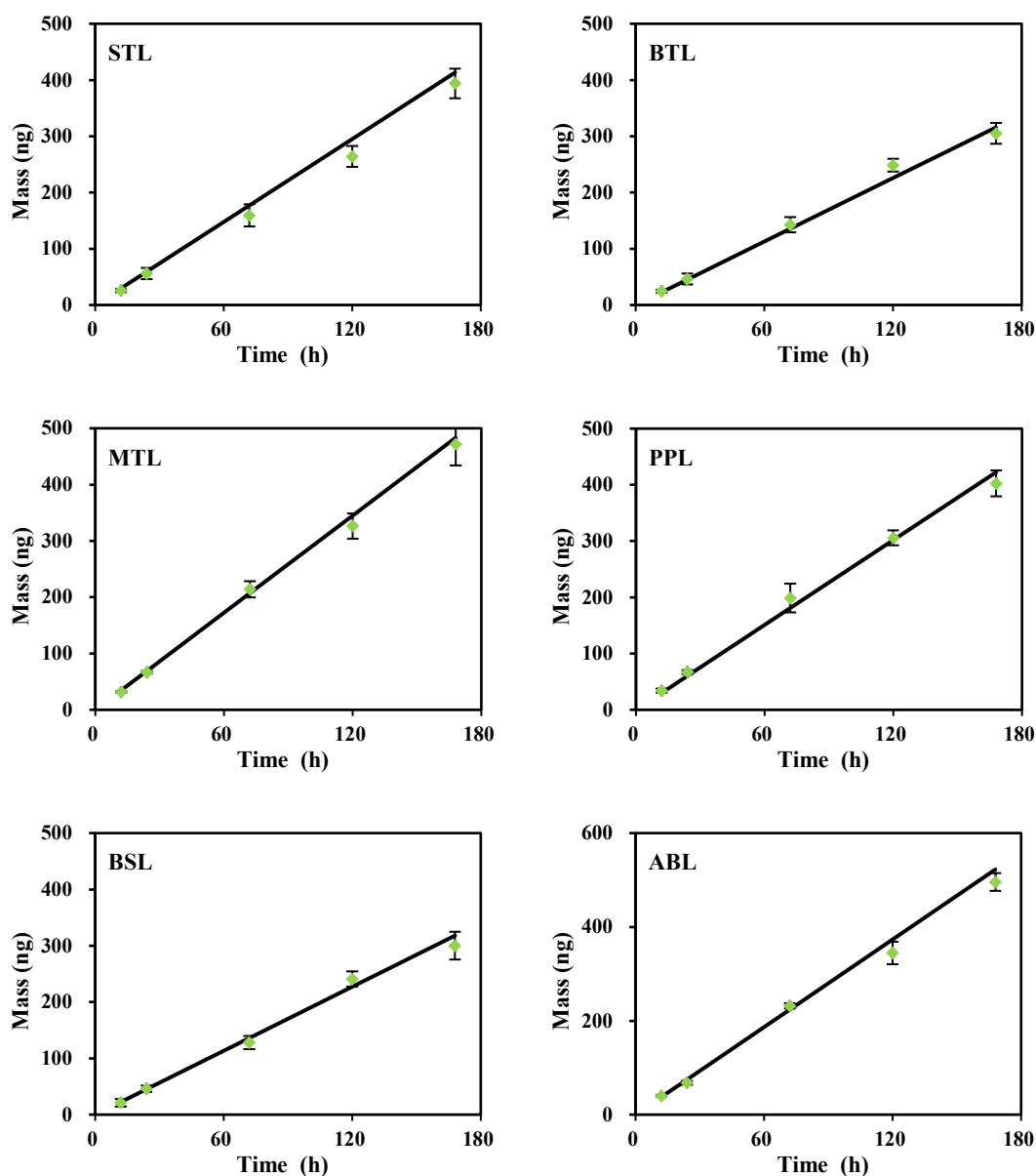
370 Several trials were carried out to obtain high and stable elution efficiencies for target  
371 compounds. For MIP binding gels immersed in solutions with  $5 \mu\text{g L}^{-1}$  mixed  
372 compounds, when ultrasonic elution was conducted once with 5 mL 5%NH<sub>3</sub> in MeOH,  
373 most of the  $\beta$ -blockers were eluted over 90% from binding gels, much higher than using  
374 ACN or 10%HAc in MeOH, except for BTL and PPL with only ~65% (shown in Table  
375 S6). To improve the elution efficiencies for all target compounds, elution processes  
376 were carried out twice sequentially with 3 mL eluant each time. The recoveries of all  
377 target compounds were over 85% using 10% HAc in MeOH. Therefore, this double  
378 elution procedure was adopted for the following experiments. The elution efficiencies  
379 were further tested for lower concentration of target compounds in solutions of  $0.5 \mu\text{g}$   
380  $\text{L}^{-1}$ . The results were similar to those obtained for higher concentrations when using  
381 10%HAc in MeOH (Table S6).

382 The detection limits of MIP-DGT for target  $\beta$ -blockers were within the range from 0.5  
383 –  $1.6 \text{ ng L}^{-1}$  in a 7-day deployment (shown in Table S4), which can meet the requirement  
384 for detecting low concentrations of target  $\beta$ -blockers in WWTPs.

### 385 3.5 Time and diffusive layer thickness dependence

386 Two laboratory experiments were carried out to validate the principle of DGT for  
387 measuring  $\beta$ -blocker drugs. Multiple DGT devices were deployed in mixed-compound  
388 solution at  $5 \mu\text{g L}^{-1}$  to test the relationship between uptake mass and deployment time.  
389 As shown in Fig. 5, the accumulation of all target compounds increased linearly with  
390 the deployment time up to 168 h. The uptake of 7 compounds agreed well with  
391 theoretical predictions, except for ATL, which displayed deviations from the theoretical  
392 line. It was reported that the linear uptake of ATL went on for only 4 days in a  $5 \mu\text{g L}^{-1}$   
393 solution with 30 mixed compounds using DGT with HLB resin [51]. The poor uptake  
394 of ATL could be caused by the competitive adsorption between target compounds. In  
395 our study, although the binding material was selective, ATL still competed with the  
396 other  $\beta$ -blockers. This phenomenon could also be reflected from the slow uptake rate  
397 of ATL compared to other target  $\beta$ -blockers in the effective capacity experiment.  
398 However, after 7 days, 86% of the predicted mass of ATL was detected, which was still  
399 acceptable.





400 **Fig. 5.** Measured masses of 8 target  $\beta$ -blockers in the MIP binding layer of DGT devices  
 401 for different times. The lines are theoretical lines obtained using Eq. 1.

402 The masses of target compounds that diffuse through the diffusion layer (including  
 403 diffusive gel and filter membrane) should be inversely proportional to the diffusion  
 404 layer thickness as shown in Eq. 1 (diffusion coefficients were measured in our previous  
 405 study which is under review and shown in Table S4). Almost all the test data agreed  
 406 well with theoretical lines calculated from the test solution concentration (see Fig. S2),  
 407 showing that concentration of target compounds could be accurately measured and the  
 408 diffusion boundary layer (DBL) was insignificant under fast stirred conditions. The

409 only exception was ATL diffusing through 0.5 mm diffusive gel, for which the  
410 accumulated masses on the binding gel was ~88% of the predicted value. This may  
411 again be attributed to the lower uptake efficiency of ATL.

### 412 **3.6 DGT performance tests under different conditions**

413 In the complex wastewater environment, physicochemical properties of target  
414 compounds may change with the environment conditions and affect DGT measurement.

415 Biofilm grown on the surface of the filter membrane sometimes affects the uptake of  
416 compounds in natural waters and it may be more serious in wastewaters. The effects of  
417 pH, IS DOM and biofouling on the DGT measurement were evaluated using  $C_{DGT}/C_{soln}$   
418 ratios.

419 Most  $C_{DGT}/C_{soln}$  values were within the acceptable range (0.9 - 1.1) when pH increased  
420 from 4.58 to 8.89 (shown in Fig. 6(a)), indicating that pH had no significant effect on  
421 the measurement using DGT, satisfying most cases in wastewaters. However, when pH  
422 decreased to 3.75, the ratio of ATL and NDL dropped a little to 0.83 and 0.87. This may  
423 due to the slightly less efficient and less effective uptake of these two compounds to  
424 MIP binding gel at more acidic pH range. Similar decreasing trends were observed for  
425 ATL detection using HLB-DGT. Adsorption significantly declined from pH 8.5 to pH  
426 5 [51]. Several studies found negative effects of high pH on the performance of DGT  
427 measuring EDCs using SXLA resin gels [18], pesticides by HLB resin gels [52], and  
428 tetrabromobisphenol A through MIP binding gels [30]. Comparing to these widely used  
429 resins, performance of MIP-DGT was more resistant to extreme pH environmental  
430 conditions.

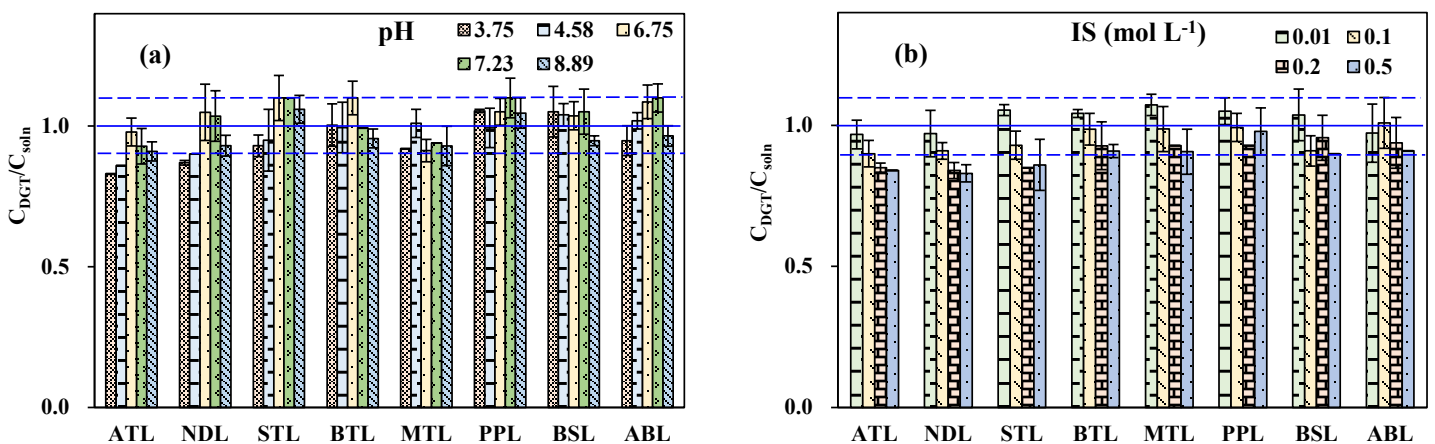
431 As presented in Fig. 6(b), a slight reduction of  $C_{DGT}/C_{soln}$  values was observed for most  
432 target compounds when the IS increased from 0.01 to 0.5 M, but most of them still fell  
433 into the range 0.9 – 1.1. For ATL, NDL and STL, the ratio values dropped to ~0.85

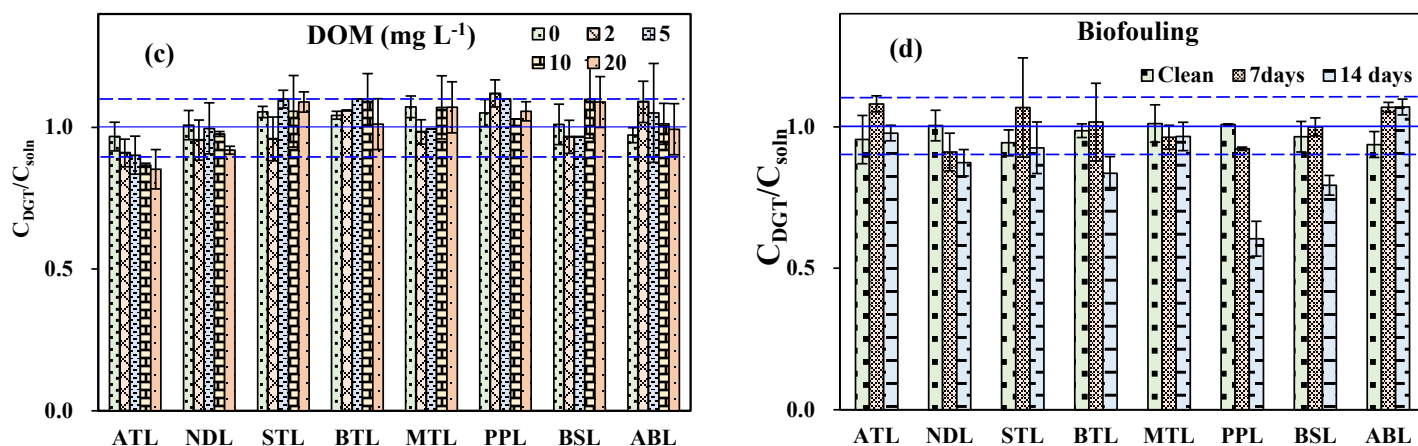
434 when the IS was 0.2 M. The effect of IS on the uptake of target compounds varied due  
435 to different mechanisms. In contrast to our study, some studies reported increasing  
436 adsorption of target compounds to the MIP adsorbent, due to the salting-out effect [53].  
437 In our study, this inhibition is compound dependent and may due to interference of mass  
438 transfer caused by the increasing salinity [54] and the competition between ionized  
439 forms of compounds [55], since these three compounds had slow uptake rates to the  
440 MIPs.

441 DOM can reduce uptake of compounds by DGT, since it may bind with target  
442 compounds, and/or compete with target compounds for adsorption sites [56]. It was  
443 reported that the adsorption of fluoroquinolone antibiotics onto MIP binding gels was  
444 greatly suppressed, for example [28]. In our study, DOM did not have obvious impacts  
445 on uptake to the DGT samplers in the range of 0 – 20 mg L<sup>-1</sup>, except for ATL, which  
446 was slightly affected by high DOM content with a  $C_{DGT}/C_{soln}$  ratio of 0.85 (shown in  
447 Fig. 6(c)). More hydrophobic compounds are more likely to adsorb to DOM. The  
448  $\log K_{ow}$  values of target  $\beta$ -blockers were all < 4, which could be defined as ‘hydrophilic’.  
449 Thus, the sampling of target  $\beta$ -blockers by MIP-DGT was independent of DOM.

450 In general, the performances of DGT devices were independent of various  
451 environmental conditions. Although the uptake of ATL was slightly inhibited (< 15%).  
452 The growth of biofilms on the surface of the filter membrane when DGT was deployed  
453 in WWTP is a consequence of exposure. The influent of WWTP is considered as a  
454 nutrient- and microorganism-rich sampling environment [57], so attention should be  
455 paid to the biofouling effect. DGT devices with PTFE filter membranes (PALL,  
456 thickness: 0.065 mm, pore size: 0.22  $\mu$ m) were deployed in the influent of a WWTP in  
457 Dalian, China for 7 and 14 days to let biofilm grow on the surface of the filter membrane.  
458 After retrieval and jet washing with MQ, new DGT devices were assembled with fouled

459 filter membranes for further experiments. As seen in Fig. S3, unlike some previous  
 460 studies where the surface of the filter membrane was covered with yellow or brown  
 461 biofilm after 10 days [58], the colour of biofilm in this study was light brown, implying  
 462 that biofilm had been built up, but any change in thickness of the filters was not  
 463 observed. As seen in Fig. 6(d),  $C_{DGT}/C_{soln}$  ratio values were still within the range of 0.9  
 464 – 1.1 with 7-day fouled filter membrane. Other studies also observed no effect of  
 465 biofouling on the DGT measurement of tetracyclines by biofilm cultivated in  
 466 wastewater < 5 days [59] and PFAS for 21 days [60]. As no systematic decrease was  
 467 observed, the change of the membrane thickness could be ignored. However, the uptake  
 468 of 3 target compounds using DGT with 14-day fouled filter membrane was suppressed,  
 469 especially for PPL, where the  $C_{DGT}/C_{soln}$  ratio dropped to 0.6. That may due to the  
 470 relatively high  $\log K_{ow}$  value (3.48) of PPL, which is consistent with the detection of  
 471 some HPCPs (BPA) and EDCs (ethylparaben and propylparaben). Although considered  
 472 as hydrophilic, some of the compounds ( $\log K_{ow} > 2.5$ ) could still be affected by  
 473 biofouling while the uptake was independent of DOM [17, 18, 61]. The results therefore  
 474 demonstrated that a 7-day (or less) deployment time for measuring  $\beta$ -blockers in the  
 475 WWTP is recommended.





477 **Fig. 6.** Effect of (a): pH; (b): ionic strength (IS); (c): dissolved organic matter (DOM);  
 478 (d): biofouling on the performance of MIP-DGTs.

### 479 3.7 Application in WWTP and estimated drug consumption through WBE

#### 480 3.7.1 Application of MIP-DGT in the WWTP

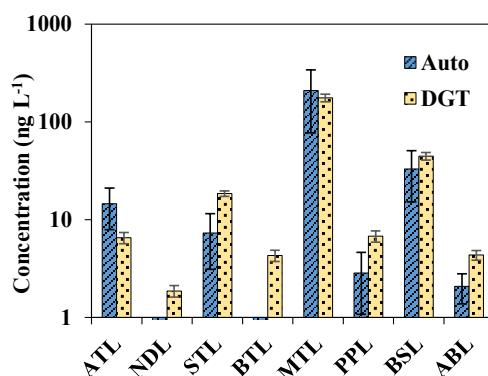
481 MIP-DGT devices were deployed at the influent of a WWTP in Dalian, China. A 24 h  
 482 daily composite water sample was collected with an autosampler alongside with DGT,  
 483 as a commonly used sampling approach for WBE (shown in Fig. S4(a-c)). The pH and  
 484 temperatures measured are listed in Table S7. All target  $\beta$ -blockers were detected using  
 485 both approaches (see Fig. 7). Concentration of MTL was an order of magnitude higher  
 486 than the other  $\beta$ -blockers in the influent, with a concentration ranging from 130 – 440  
 487 ng L<sup>-1</sup>. Usually ATL, MTL and PPL are three important  $\beta$ -blockers receiving most  
 488 attention in wastewater monitoring studies [62]. ATL and MTL together account for  
 489 more than 80% of total  $\beta$ -blocker consumption in Europe [63]. However, in our  
 490 wastewater sampling campaign, the concentration of ATL was < 20 ng L<sup>-1</sup>; PPL was  
 491 also relatively low (< 10 ng L<sup>-1</sup>), which may due to the prescription differences.



492 Concentrations of BSL were the second highest, ranging from 19 – 64 ng L<sup>-1</sup>. This was  
493 similar as the situation in some WWTPs in Serbia, where the concentrations of MTL  
494 detected was even over 700 µg L<sup>-1</sup> [64].

495 In the MIP-DGT deployment, the uptake masses of most target compounds increased  
496 gradually with the increasing deployment time in the first 5 days (shown in Fig. S5),  
497 after which a plateau or decline occurred. A similar phenomenon was observed in  
498 measuring EDCs using HLB-DGT after 18 days [18] and fluoroquinolone antibiotics  
499 by MIP-DGT after a week [28]. In our study, the rate of increase slowed after 5 days,  
500 which is mainly attributed to the sludge attached to the surface of the filter membrane  
501 as seen in Fig. S4(d). It is believed that the sludge and sand covered part of the filter  
502 membranes, impeding further uptake of target compounds. As shown earlier, the  
503 selective adsorption capacities for target compounds were much greater than the  
504 accumulated masses in this campaign, so this phenomenon is not thought to be caused  
505 by saturated adsorption of the MIP binding gels.

506 Given these observations, to avoid the underestimation of the measured concentration  
507 of target compounds, we suggest that deployment for 5 days or less is a suitable pre-  
508 cautionary approach. As Fig. 7 shows, comparable concentrations were obtained by 5-  
509 day DGT deployment to 5-day average concentration measured using the auto-sampler.  
510 The day-on-day variations in concentrations measured with the autosampler give a  
511 larger variation (standard deviations) than those measured by DGT. Thus, DGT can be  
512 used as an effective and efficient (time integrative) sampling tool for WBE.

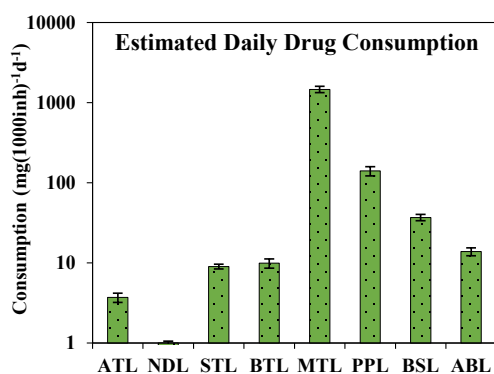


513

514 **Fig. 7.** 5-day TWA concentration measured by MIP-DGT and average concentration  
 515 of 24 h composite samples (taken each day for 5 days) for target β-blockers in the  
 516 influent of a WWTP.

### 517 3.7.2 Estimated daily drug consumption through WBE

518 Several laboratory tests have been conducted to validate the measurement of COT using  
 519 HLB-DGT. The elution efficiency of COT using 5 mL 5% NH<sub>3</sub> in MeOH was 98.6 ±  
 520 4.5 %. 3 HLB-DGT devices with PA diffusive gels and PTFE filter membranes were  
 521 immersed in a 2 L solution for 24 h to measure the diffusion coefficient of COT.  
 522 Through calculation using Eq. 1, it was 3.62 × 10<sup>-6</sup> cm<sup>2</sup> s<sup>-1</sup> at 25 °C. The detected  
 523 concentration of COT during the 5-day deployment was 1690 ± 132 ng L<sup>-1</sup>, the  
 524 discharge coefficient (*E*) of COT in Dalian was estimated as 0.7 mg d<sup>-1</sup> inh<sup>-1</sup> [65]. The  
 525 mean COT equivalent population (*P*<sub>COT</sub>) was calculated as 157 ± 12 (× 10<sup>3</sup>) in the  
 526 WWTP. According to Eq. 6, the estimated daily consumptions of different target β-  
 527 blockers varied greatly as shown in Fig, 8, ranging from 0.9 (NDL) to 1463 (MTL) mg  
 528 (1000 inh)<sup>-1</sup> d<sup>-1</sup>, indicating that β-blocker drugs such as MTL and PPL (140 mg (1000  
 529 inh)<sup>-1</sup> d<sup>-1</sup>) are still the most prescribed cardiovascular drugs, accounting for > 95% of  
 530 the total consumption. The extremely high consumption of MTL was consistent with  
 531 the situation in most parts of China [65], as it had a high utilization rate for hypertension  
 532 patients.



533 **Fig. 8.** Estimated daily consumption of target  $\beta$ -blockers per 1000 people

534 **4. Conclusion**

535 A new DGT device based on MIP with high selectivity for  $\beta$ -blocker drugs was  
 536 developed for accurate measurement of those compounds in wastewater. The MIP  
 537 binding material synthesized by polymerization had strong affinity and a large effective  
 538 capacity to target compounds. The performances of MIP-DGT for most target  
 539 compounds were independent of pH (in the range 4.58 – 8.89), ionic strength (0.01 –  
 540 0.5 M), DOM (< 20mg L<sup>-1</sup>), with only ATL as an exception, but the accuracies were  
 541 still acceptable (< 15% errors). The uptake of all target compounds was not affected by  
 542 biofilm grown for 7 days, which ensured the reliable sampling and measurement of  $\beta$ -  
 543 blockers in WWTP. During the sampling campaign in the influent of a WWTP, all target  
 544 compounds were detectable. The calculation based on MIP-DGT data showed that MTL  
 545 and PPL were the two most popular cardiovascular drugs in the studied area.

546 Comparing to HLB resin and commercial MIP material (~\$270/g) which is no longer  
 547 in the market, the MIP material synthesized in this study has economic benefits with  
 548 the cost < \$20/g. The detection limit of DGT devices in field deployment can reach 0.5  
 549 – 1.6 ng L<sup>-1</sup> for target  $\beta$ -blocker drugs, which could meet the demand for wastewater  
 550 monitoring. It preconcentrates target compounds *in situ*, reduces the treatment  
 551 procedures in the laboratory, saves labour and time. Therefore, compared to

552 conventional auto-sampling, DGT has advantages in cost, time integration, efficiency  
553 and detection limit, making it an ideal tool for wastewater surveillance.

554

#### 555 **Notes**

556 The authors declare no conflict of interest.

#### 557 **CRedit authorship contribution statement**

558 Yanying Li: Investigation, Project administration, Writing – original draft. Mingzhe

559 Wu: Investigation, Methodology. Xinyu Yin: Methodology, Validation. Yansong

560 Wang: Methodology. Dongqin Tan: Methodology, Funding acquisition. Peng Zhang:

561 Data curation, Funding acquisition. Zhimin Zhou: Funding acquisition, Validation.

562 Degao Wang: Conceptualization, Supervision. Kevin C. Jones: Supervision, Writing –

563 review & editing. Hao Zhang: Supervision, Writing – review & editing.

#### 564 **Declaration of competing interest**

565 The authors declare that they have no known competing financial interests or personal

566 relationships that could have appeared to influence the work reported in this paper.

#### 567 **Data availability**

568 Data will be made available on request.

#### 569 **Acknowledgement**

570 This work was supported by Dalian Key Research and Development Plan (No.

571 2023YF23WZ046), the Open Foundation of Key Laboratory of Industrial Ecology and

572 Environmental Engineering MOE (KLIEEE-23-05), and the National Natural Science

573 Foundation of China (No. 22076112).

#### 574 **Supporting Information**

575 Supplementary data associated with this article can be found in the online version at

576

577 **References**

- 578 [1] Li, Z., Li, J., Hu, Y., Yan, Y., Tang, S., Ma, R., Li, L., 2024. Evaluation of pharmaceutical consumption  
579 between urban and suburban catchments in China by wastewater-based epidemiology.  
580 *Environmental Research* 118544.
- 581 [2] Li, Y., Ash, K.T., Williams, D.E., Hazen, T.C., 2023. Evaluating various composite sampling modes  
582 for detecting pathogenic SARS-CoV-2 virus in raw sewage. *Frontiers in microbiology* 14 1305967.
- 583 [3] Mendoza Grijalva, L., Brown, B., Cauble, A., Tarpeh, W.A., 2022. Diurnal variability of SARS-CoV-  
584 2 RNA concentrations in hourly grab samples of wastewater influent during low COVID-19  
585 incidence. *ACS Es&t Water* 2 (11), 2125-2133.
- 586 [4] König, A.W., Ariano, S.S., Joksimovic, D., 2023. Analysis of sampling strategies for pulse loads  
587 of SARS-CoV-2: Implications for wastewater-based epidemiology. *Water Science & Technology*  
588 88 (4), 1039-1057.
- 589 [5] Liang, Y., Li, H., Li, S., Chen, S., 2023. Organic diffusive gradients in thin films (o-DGT) for  
590 determining environmental behaviors of antibiotics: A review. *Journal of Hazardous Materials*  
591 132279.
- 592 [6] Hahn, R.Z., Augusto do Nascimento, C., Linden, R., 2021. Evaluation of illicit drug consumption  
593 by wastewater analysis using polar organic chemical integrative sampler as a monitoring tool.  
594 *Frontiers in Chemistry* 9 596875.
- 595 [7] Lizot, L.d.L.F., Bastiani, M.F., Hahn, R.Z., Meireles, Y.F., Freitas, M., Bondan, A.P., do Nascimento,  
596 C.A., Quevedo, D.M., Linden, R., 2023. Risk assessment of a Brazilian urban population due to the  
597 exposure to pyrethroid insecticides during the COVID-19 pandemic using wastewater-based  
598 epidemiology. *Chemosphere* 345 140526.
- 599 [8] Parkins, M.D., Lee, B.E., Acosta, N., Bautista, M., Hubert, C.R., Hruday, S.E., Frankowski, K., Pang,  
600 X.-L., 2023. Wastewater-based surveillance as a tool for public health action: SARS-CoV-2 and  
601 beyond. *Clinical Microbiology Reviews* 37 e00103-00122.
- 602 [9] Xie, H., Dong, Y., Chen, J., Wang, X., Fu, M., 2021. Development and evaluation of a ceramic  
603 diffusive layer based DGT technique for measuring organic micropollutants in seawaters.  
604 *Environment International* 156 106653.
- 605 [10] de Barros, R.M., Rougerie, J., Guibal, R., Lissalde, S., Buzier, R., Simon, S., Guibaud, G., 2023.  
606 Interest of a new large diffusive gradients in thin films (L-DGT) for organic compounds monitoring:  
607 On-field comparison with conventional passive samplers. *Environmental Pollution* 323 121257.
- 608 [11] Criquet, J., Dumoulin, D., Howsam, M., Mondamert, L., Goossens, J.-F., Prygiel, J., Billon, G.,  
609 2017. Comparison of POCIS passive samplers vs. composite water sampling: a case study. *Science  
610 of the Total Environment* 609 982-991.
- 611 [12] Terzopoulou, E., Voutsas, D., 2016. Active and passive sampling for the assessment of  
612 hydrophilic organic contaminants in a river basin-ecotoxicological risk assessment. *Environmental  
613 Science and Pollution Research* 23 5577-5591.
- 614 [13] Buzier, R., Guibal, R., Lissalde, S., Guibaud, G., 2019. Limitation of flow effect on passive  
615 sampling accuracy using POCIS with the PRC approach or o-DGT: a pilot-scale evaluation for  
616 pharmaceutical compounds. *Chemosphere* 222 628-636.
- 617 [14] Trommetter, G., Dumoulin, D., Billon, G., 2021. Development and validation of DGT passive  
618 samplers for the quantification of Ir, Pd, Pt, Rh and Ru: A challenging application in waters  
619 impacted by urban activities. *Talanta* 223 121707.
- 620 [15] Chen, C.-E., Zhang, H., Jones, K.C., 2012. A novel passive water sampler for in situ sampling

621 of antibiotics. *Journal of Environmental Monitoring* 14 (6), 1523-1530.

622 [16] Fang, Z., Li, Y., Li, Y., Yang, D., Zhang, H., Jones, K.C., Gu, C., Luo, J., 2021. Development and  
623 applications of novel DGT passive samplers for measuring 12 per-and polyfluoroalkyl substances  
624 in natural waters and wastewaters. *Environmental Science & Technology* 55 (14), 9548-9556.

625 [17] Chen, W., Li, Y., Chen, C., Sweetman, A., Zhang, H., Jones, K., 2017. DGT passive sampling for  
626 quantitative in situ measurements of compounds from household and personal care products in  
627 waters. *Environmental Science & Technology* 51 (22), 13274-13281.

628 [18] Chen, W., Pan, S., Cheng, H., Sweetman, A.J., Zhang, H., Jones, K.C., 2018. Diffusive gradients  
629 in thin-films (DGT) for in situ sampling of selected endocrine disrupting chemicals (EDCs) in waters.  
630 *Water Research* 137 211-219.

631 [19] Ren, S., Tan, F., Wang, Y., Zhao, H., Zhang, Y., Zhai, M., Chen, J., Wang, X., 2020. In situ  
632 measurement of synthetic musks in wastewaters using diffusive gradients in thin film technique.  
633 *Water Research* 185 116239.

634 [20] Liu, X., Zhang, R., Cheng, H., Khorram, M.S., Zhao, S., Tham, T.T., Tran, T.M., Minh, T.B., Jiang,  
635 B., Jin, B., 2021. Field evaluation of diffusive gradients in thin-film passive samplers for wastewater-  
636 based epidemiology. *Science of the Total Environment* 773 145480.

637 [21] Li, Y., Chen, C.-E.L., Chen, W., Chen, J., Cai, X., Jones, K.C., Zhang, H., 2019. Development of a  
638 passive sampling technique for measuring pesticides in waters and soils. *Journal of Agricultural  
639 and Food Chemistry* 67 (22), 6397.

640 [22] Guo, C., Zhang, T., Hou, S., Lv, J., Zhang, Y., Wu, F., Hua, Z., Meng, W., Zhang, H., Xu, J., 2017.  
641 Investigation and application of a new passive sampling technique for in situ monitoring of illicit  
642 drugs in waste waters and rivers. *Environmental Science & Technology* 51 (16), 9101-9108.

643 [23] Xie, H., Chen, J., Chen, Q., Chen, C.-E.L., Du, J., Tan, F., Zhou, C., 2018. Development and  
644 evaluation of diffusive gradients in thin films technique for measuring antibiotics in seawater.  
645 *Science of the Total Environment* 618 1605-1612.

646 [24] Yan, L., Rong, Q., Zhang, H., Jones, K.C., Li, Y., Luo, J., 2022. Evaluation and Application of a  
647 Novel Diffusive Gradients in Thin-Films Technique for In Situ Monitoring of Glucocorticoids in  
648 Natural Waters. *Environmental Science & Technology* 56 (22), 15499-15507.

649 [25] Zou, Y.-T., Fang, Z., Li, Y., Wang, R., Zhang, H., Jones, K.C., Cui, X.-Y., Shi, X.-Y., Yin, D., Li, C.,  
650 2018. Novel Method for in Situ Monitoring of Organophosphorus Flame Retardants in Waters.  
651 *Analytical Chemistry* 90 (16), 10016-10023.

652 [26] Hu, Y., Muhammad, T., Wu, B., Wei, A., Yang, X., Chen, L., 2020. A simple on-line detection  
653 system based on fiber-optic sensing for the realtime monitoring of fixed bed adsorption processes  
654 of molecularly imprinted polymers. *Journal of Chromatography A* 1622 461112.

655 [27] Chen, L., Wang, X., Lu, W., Wu, X., Li, J., 2016. Molecular imprinting: perspectives and  
656 applications. *Chemical society reviews* 45 (8), 2137-2211.

657 [28] Liu, S.-S., Li, J.-L., Ge, L.-K., Li, C.-L., Zhao, J.-L., Zhang, Q.-Q., Ying, G.-G., Chen, C.-E., 2021.  
658 Selective diffusive gradients in thin-films with molecularly imprinted polymer for measuring  
659 fluoroquinolone antibiotics in waters. *Science of the Total Environment* 790 148194.

660 [29] Cui, Y., Tan, F., Wang, Y., Ren, S., Chen, J., 2020. Diffusive gradients in thin films using  
661 molecularly imprinted polymer binding gels for in situ measurements of antibiotics in urban  
662 wastewaters. *Frontiers of Environmental Science & Engineering* 14 1-12.

663 [30] Feng, Z., Wang, Y., Yang, L., Sun, T., 2019. Coupling mesoporous imprinted polymer based  
664 DGT passive samplers and HPLC: A new tool for in-situ selective measurement of low

665 concentration tetrabromobisphenol A in freshwaters. *Science of the Total Environment* 685 442-  
666 450.

667 [31] Zhu, Y., Xu, G., Wang, X., Ji, X., Jia, X., Sun, L., Gu, X., Xie, X., 2022. Passive sampling of  
668 chlorophenols in water and soils using diffusive gradients in thin films based on  $\beta$ -cyclodextrin  
669 polymers. *Science of the Total Environment* 806 150739.

670 [32] Dong, J., Fan, H., Sui, D., Li, L., Sun, T., 2014. Sampling 4-chlorophenol in water by DGT  
671 technique with molecularly imprinted polymer as binding agent and nylon membrane as diffusive  
672 layer. *Analytica Chimica Acta* 822 69-77.

673 [33] Rong, Q., Li, Y., Luo, J., Yan, L., Jones, K.C., Zhang, H., 2024. Development of a novel DGT  
674 passive sampler for measuring polycyclic aromatic hydrocarbons in aquatic systems. *Journal of*  
675 *Hazardous Materials* 470 134199.

676 [34] Pathak, A., Mrabeti, S., 2021.  $\beta$ -Blockade for patients with hypertension, ischemic heart disease  
677 or heart failure: Where are we now? *Vascular Health and Risk Management* 17 337-348.

678 [35] Gao, Y.-q., Gao, N.-y., Chen, J.-x., Zhang, J., Yin, D.-q., 2020. Oxidation of  $\beta$ -blocker atenolol  
679 by a combination of UV light and chlorine: kinetics, degradation pathways and toxicity assessment.  
680 *Separation and Purification Technology* 231 115927.

681 [36] Ma, R., Qu, H., Wang, B., Wang, F., Yu, G., 2020. Widespread monitoring of chiral  
682 pharmaceuticals in urban rivers reveals stereospecific occurrence and transformation. *Environment*  
683 *International* 138 105657.

684 [37] Yi, M., Sheng, Q., Sui, Q., Lu, H., 2020.  $\beta$ -blockers in the environment: Distribution,  
685 transformation, and ecotoxicity. *Environmental Pollution* 266 115269.

686 [38] Aydın, S., Ulvi, A., Bedük, F., Aydın, M.E., 2022. Pharmaceutical residues in digested sewage  
687 sludge: Occurrence, seasonal variation and risk assessment for soil. *Science of the Total*  
688 *Environment* 817 152864.

689 [39] Huggett, D., Brooks, B., Peterson, B., Foran, C., Schlenk, D., 2002. Toxicity of select beta  
690 adrenergic receptor-blocking pharmaceuticals (B-blockers) on aquatic organisms. *Archives of*  
691 *Environmental Contamination and Toxicology* 43 (2), 229-235.

692 [40] Khan, B., Burgess, R.M., Fogg, S.A., Cantwell, M.G., Katz, D.R., Ho, K.T., 2018. Cellular responses  
693 to in vitro exposures to  $\beta$ -blocking pharmaceuticals in hard clams and Eastern oysters.  
694 *Chemosphere* 211 360-370.

695 [41] Bayati, M., Ho, T.L., Vu, D.C., Wang, F., Rogers, E., Cuvelier, C., Huebotter, S., Inniss, E.C.,  
696 Udawatta, R., Jose, S., 2021. Assessing the efficiency of constructed wetlands in removing PPCPs  
697 from treated wastewater and mitigating the ecotoxicological impacts. *International Journal of*  
698 *Hygiene and Environmental Health* 231 113664.

699 [42] Gros, M., Pizzolato, T.-M., Petrović, M., de Alda, M.J.L., Barceló, D., 2008. Trace level  
700 determination of  $\beta$ -blockers in waste waters by highly selective molecularly imprinted polymers  
701 extraction followed by liquid chromatography–quadrupole-linear ion trap mass spectrometry.  
702 *Journal of Chromatography A* 1189 (1-2), 374-384.

703 [43] Miège, C., Budzinski, H., Jacquet, R., Soulier, C., Pelte, T., Coquery, M., 2012. Polar organic  
704 chemical integrative sampler (POCIS): application for monitoring organic micropollutants in  
705 wastewater effluent and surface water. *Journal of Environmental Monitoring* 14 (2), 626-635.

706 [44] Challis, J.K., Hanson, M.L., Wong, C.S., 2016. Development and calibration of an organic-  
707 diffusive gradients in thin films aquatic passive sampler for a diverse suite of polar organic  
708 contaminants. *Analytical Chemistry* 88 (21), 10583-10591.

709 [45] Hou, H., Jin, Y., Sheng, L., Huang, Y., Zhao, R., 2022. One-step synthesis of well-defined  
710 molecularly imprinted nanospheres for the class-selective recognition and separation of  $\beta$ -  
711 blockers in human serum. *Journal of Chromatography A* 1673 463204.

712 [46] Gao, J., Li, J., Jiang, G., Yuan, Z., Eaglesham, G., Covaci, A., Mueller, J.F., Thai, P.K., 2018. Stability  
713 of alcohol and tobacco consumption biomarkers in a real rising main sewer. *Water Research* 138  
714 19-26.

715 [47] Rico, M., Andrés-Costa, M.J., Picó, Y., 2017. Estimating population size in wastewater-based  
716 epidemiology. Valencia metropolitan area as a case study. *Journal of Hazardous Materials* 323  
717 156-165.

718 [48] Hasanah, A.N., Susanti, I., Mutakin, M., 2022. An update on the use of molecularly imprinted  
719 polymers in beta-blocker drug analysis as a selective separation method in biological and  
720 environmental analysis. *Molecules* 27 (9), 2880.

721 [49] Gorbani, Y., Yilmaz, H., Basan, H., 2017. Spectrofluorimetric determination of atenolol from  
722 human urine using high - affinity molecularly imprinted solid - phase extraction sorbent.  
723 *Luminescence* 32 (8), 1391-1397.

724 [50] Pratiwi, R., Megantara, S., Rahayu, D., Pitaloka, I., Hasanah, A.N., 2019. Comparison of bulk  
725 and precipitation polymerization method of synthesis molecular imprinted solid phase extraction  
726 for atenolol using methacrylic acid. *Journal of Young Pharmacists* 11 (1), 12.

727 [51] Stroski, K.M., Challis, J.K., Wong, C.S., 2018. The influence of pH on sampler uptake for an  
728 improved configuration of the organic-diffusive gradients in thin films passive sampler. *Analytica*  
729 *Chimica Acta* 1018 45-53.

730 [52] Guibal, R., Buzier, R., Charriau, A., Lissalde, S., Guibaud, G., 2017. Passive sampling of anionic  
731 pesticides using the Diffusive Gradients in Thin films technique (DGT). *Analytica Chimica Acta* 966  
732 1-10.

733 [53] Yu, Q., Deng, S., Yu, G., 2008. Selective removal of perfluorooctane sulfonate from aqueous  
734 solution using chitosan-based molecularly imprinted polymer adsorbents. *Water Research* 42 (12),  
735 3089-3097.

736 [54] Semple, K., Morriss, A., Paton, G., 2003. Bioavailability of hydrophobic organic contaminants  
737 in soils: fundamental concepts and techniques for analysis. *European Journal of Soil Science* 54 (4),  
738 809-818.

739 [55] Jeong, Y., Schäffer, A., Smith, K., 2017. Equilibrium partitioning of organic compounds to  
740 OASIS HLB® as a function of compound concentration, pH, temperature and salinity.  
741 *Chemosphere* 174 297-305.

742 [56] Godlewska, K., Jakubus, A., Stepnowski, P., Paszkiewicz, M., 2021. Impact of environmental  
743 factors on the sampling rate of  $\beta$ -blockers and sulfonamides from water by a carbon nanotube-  
744 passive sampler. *Journal of Environmental Sciences* 101 413-427.

745 [57] McLellan, S., Huse, S.M., Mueller-Spitz, S., Andreishcheva, E., Sogin, M., 2010. Diversity and  
746 population structure of sewage-derived microorganisms in wastewater treatment plant influent.  
747 *Environmental microbiology* 12 (2), 378-392.

748 [58] Feng, Z., Zhang, W., Sun, T., 2021. Effects of seasonal biofouling on diffusion coefficients  
749 through filter membranes with different hydrophilicities in natural waters. *Science of the Total*  
750 *Environment* 794 148536.

751 [59] You, N., Yao, H., Wang, Y., Fan, H.-T., Wang, C.-S., Sun, T., 2019. Development and evaluation  
752 of diffusive gradients in thin films based on nano-sized zinc oxide particles for the in situ sampling



753 of tetracyclines in pig breeding wastewater. *Science of the Total Environment* 651 1653-1660.

754 [60] Wang, P., Challis, J.K., He, Z.-X., Wong, C.S., Zeng, E.Y., 2022. Effects of biofouling on the  
755 uptake of perfluorinated alkyl acids by organic-diffusive gradients in thin films passive samplers.  
756 *Environmental Science: Processes & Impacts* 24 (2), 242-251.

757 [61] Wang, R., Jones, K.C., Zhang, H., 2020. Monitoring organic pollutants in waters using the  
758 diffusive gradients in the thin films technique: investigations on the effects of biofouling and  
759 degradation. *Environmental Science & Technology* 54 (13), 7961-7969.

760 [62] Zhang, H., Ihara, M.O., Nakada, N., Tanaka, H., Ihara, M., 2020. Biological activity-based  
761 prioritization of pharmaceuticals in wastewater for environmental monitoring: G protein-coupled  
762 receptor inhibitors. *Environmental Science & Technology* 54 (3), 1720-1729.

763 [63] Alder, A.C., Schaffner, C., Majewsky, M., Klasmeier, J., Fenner, K., 2010. Fate of  $\beta$ -blocker  
764 human pharmaceuticals in surface water: Comparison of measured and simulated concentrations  
765 in the Glatt Valley Watershed, Switzerland. *Water Research* 44 (3), 936-948.

766 [64] Jauković, Z.D., Grujić, S.D., Vasiljević, T.M., Petrović, S.D., Laušević, M.D., 2014. Cardiovascular  
767 drugs in environmental waters and wastewaters: Method optimization and real sample analysis.  
768 *Journal of AOAC International* 97 (4), 1167-1174.

769 [65] Hou, C., Zhong, Y., Zhang, L., Liu, M., Yan, F., Chen, M., Wang, Y., Xu, P., Su, M., Hu, C., 2023.  
770 Estimating the prevalence of hypertension in 164 cities in China by wastewater-based  
771 epidemiology. *Journal of Hazardous Materials* 443 130147.

772